Nonreciprocity and one-way topological transitions in hyperbolic metamaterials

A. Leviyev[1], B. Stein[1], A. Christofi[2], T. Galfsky[1,3,4], H. Krishnamoorthy[1,4], I. L. Kuskovsky[1,4], V. Menon[1,3,4], A. B. Khanikaev[2,4*]

[1]*Department of Physics, Queens College of The City University of New York, Queens, New York 11367, USA*
[2]*Department of Electrical Engineering, City College of The City University of New York, New York, NY 10031, USA*
[3]*Department of Physics, City College of The City University of New York, New York, NY 10031, USA*
[4]*The Graduate Center of The City University of New York, New York, New York 10016, USA*
**e-mail address: akhanikaev@ccny.cuny.edu*

Control of the electromagnetic waves in nano-scale structured materials is crucial to the development of next generation photonic circuits and devices. In this context, hyperbolic metamaterials, where elliptical isofrequency surfaces are morphed into surfaces with exotic hyperbolic topologies when the structure parameters are tuned, have shown unprecedented control over light propagation and interaction. Here we show that such topological transitions can be even more unusual when the hyperbolic metamaterial is endowed with nonreciprocity. Judicious design of metamaterials with reduced spatial symmetries, together with the breaking of time-reversal symmetry through magnetization, is shown to result in nonreciprocal dispersion and one-way topological phase transitions in hyperbolic metamaterials.

Introduction. Optical metamaterials are artificial media with engineered electromagnetic response, that can be realized through subwavelength structuring, facilitate properties normally limited or not found in naturally occurring materials.[1-6] One such property is optical nonreciprocity – a rare and generally weak characteristic of light to differentiate between opposite propagation directions.[7-8] This property, which exists in magnetic materials such as ferrites, is of immense importance for devices such as optical isolators and circulators, which are widely used to stabilize laser operations and to route signals in optical telecommunication networks.[9-11] Therefore, nonreciprocal optical components are of significant interest for optical integration, which can be achieved by combining magneto-optical (MO) materials with resonant nanophotonic[12-17] and plasmonic[18-26] structures. Such integration also allows enhancement of generally weak MO response of ferrites through strong light-matter interactions in photonic[12-17] and plasmonic[18-26] nanostructures, and metamaterials.[27]

Metamaterials with magnetic constituents have been used to achieve negative index of refraction and tunable response in external magnetic field.[28-33] However, very little is known on the nonreciprocal effects that can be engineered using magnetic metamaterials.[27] In this context, hyperbolic metamaterials (HMMs),[34-44,31] a class of metamaterials with hyperbolic isofrequency contours, known for their ability to enhance light-matter interaction over a broad spectral range, including for broadband asymmetric[45] but reciprocal[46] scattering, can be exceptional candidates for novel devices, offering both enhanced nonreciprocal effects and broadband operation which are unattainable with other classes of metamaterials. In this Letter, we demonstrate that HMMs with MO activity exhibit unprecedented nonreciprocal characteristics such as one-way topological transitions[43] and one-way hyperbolic dispersion regimes.

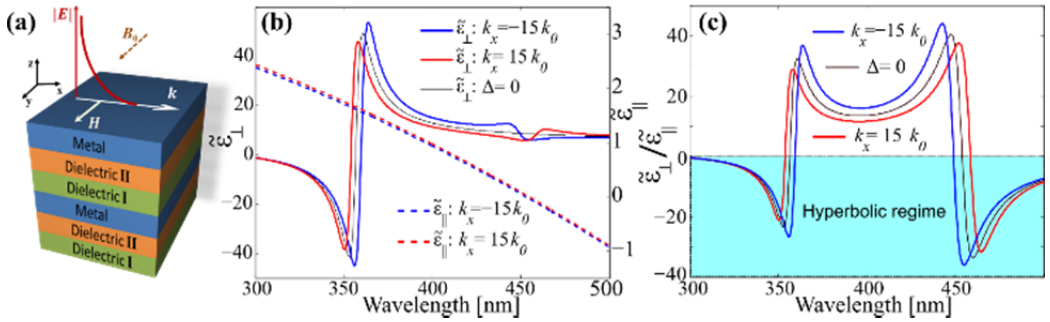

FIG. 1 (color online). (a) Schematics of three-layer nonreciprocal metamaterial and the magnetization geometry (dashed brown arrow). (b)-(c) Effective permittivities calculated from Eqs. 2(a-b) for TiO_2/Ag/SiO_2 nonreciprocal HMM. Blue and red lines: forward ($k_x > 0$) and backward ($k_x < 0$) propagation, respectively. Black lines: nonmagnetic (reciprocal) effective medium theory. Structure parameters: 14nm-thick TiO_2 with

$n_1 = 2.56$, 20nm-thick silver with ϵ_∞ =4.09, ω_p =1.33×10[16] [rad/s], γ =1.13×10[14][rad/s], and MO parameter $\Delta_2 = 0.1\epsilon_2$, and 14 nm-thick SiO_2 with $n_3 = 1.46$.

Theoretical approach and model. Optical nonreciprocity occurs only when an optical system lacks both time-reversal symmetry and inversion symmetry.[13,15,16] In the particular case of layered media magnetized in the Voigt geometry, such as photonic crystals or HMMs studied here (Fig. 1(a)), nonreciprocity can be achieved for p-polarized light either through inhomogeneous magnetization[15] or multilayered configuration.[16] Here we consider a multilayered HMM, which is easy to implement experimentally. The metamaterial is formed by periodically stacking unit cells consisting of a plasmonic ($\epsilon_2 < 0$) layer sandwiched in between two dielectric ($\epsilon_1 \neq \epsilon_3$, $\epsilon_1 > 0$, $\epsilon_3 > 0$) layers of thicknesses $a_{1,2,3}$, with the net lattice constant $a_0 = a_1 + a_2 + a_3$. The structure is subject to a DC magnetic field $\boldsymbol{B}_0$ along the y-direction and the plasmonic material is characterized by a dielectric permittivity tensor $\hat{\epsilon}_2 = [\epsilon_2, 0, i\Delta_2; 0, \epsilon_{2,yy}, 0; -i\Delta_2, 0, \epsilon_2]$,[20] where $\epsilon_2 = \epsilon_\infty - \frac{\omega_p^2}{(\omega+i\gamma)^2-\omega_B^2} \times \left(1 + i\frac{\gamma}{\omega}\right)$, $\Delta_2 = i\frac{\omega_B}{\omega} \times \frac{\omega_p^2}{(\omega+i\gamma)^2-\omega_B^2}$, $\epsilon_{2,yy} = \epsilon_\infty - \frac{\omega_p^2}{\omega(\omega+i\gamma)}$, ϵ_∞ is the high-frequency permittivity, ω_p is the bulk plasma frequency, γ is the damping frequency, $\omega_B = \frac{e}{m^*}B$ is the cyclotron frequency, and e and m^* are the charge and the effective mass of the electron, respectively. It is worth noting that strong nonreciprocity (large values of Δ_2) in metals requires strong DC magnetic fields on the order of several tesla.[20] Importantly, the nonreciprocal regimes reported here will also occur in HMMs made of highly doped semiconductors[36] in terahertz and infrared spectral domains for lower values of applied DC magnetic fields. The corresponding design of nonreciprocal hyperbolic metamaterials made of doped semiconductor and operating in mid-IR domain is presented in Supplementary Materials (section 2).[47] Moreover, in structures made of ferrites[12-19] the same effects can be achieved for magnetic fields of a few hundred Gauss, which is sufficient to provide saturation magnetization.

Nonreciprocal effective medium theory. Starting with the exact transfer matrix technique, we develop an analytic effective medium theory with nonreciprocal corrections induced by the magnetization.[47] For reciprocal structures ($\Delta_2 = 0$), this procedure results in the well-known expression $K_z^2/\epsilon_\parallel + k_x^2/\epsilon_\perp = k_0^2$, where $\epsilon_\parallel = \epsilon_1 f_1 + \epsilon_2 f_2 + \epsilon_3 f_3$ and $\epsilon_\perp = (f_1/\epsilon_1 + f_2/\epsilon_2 + f_3/\epsilon_3)^{-1}$ are the effective permittivities parallel and perpendicular to the layers, respectively, and $f_m = a_m/a_0$ is the volume fraction of the m-th layer. By applying a similar procedure to the magnetized structure, we end up with two additional terms that are odd with respect to the wavenumber:

$$\frac{K_z^{\,2}}{\epsilon_\parallel} + \frac{k_x^2}{\epsilon_\perp} + k_x^3 a_0 \frac{\Delta_2}{\epsilon_2}\frac{f_1 f_2 f_3}{\epsilon_\parallel}\left(\frac{\epsilon_3}{\epsilon_1} - \frac{\epsilon_1}{\epsilon_3}\right) = k_0^2\left[1 + k_x a_0 \frac{f_1 f_2 f_3}{\epsilon_\parallel}\frac{\Delta_2}{\epsilon_2}(\epsilon_3 - \epsilon_1)\right]. \quad (1)$$

In the reciprocal case such odd-order terms in k_x do not appear and the next term would be of fourth order, which is the direct consequence of the reciprocity $k_0(\boldsymbol{k}) = k_0(-\boldsymbol{k})$ [or $\omega(\boldsymbol{k}) = \omega(-\boldsymbol{k})$]. This condition is clearly not satisfied for Eq. (1) where the two additional terms, linear and cubic with respect to k_x, lead to the nonreciprocal dispersion $k_0(\boldsymbol{k}) \neq k_0(-\boldsymbol{k})$. One can see from Eq. (1) that these nonreciprocal terms increase with the MO parameter Δ_2 and/or the dielectric contrast between two layers adjacent to the magneto-plasmonic layer. The latter dependence confirms that for the inversion symmetric and bilayer structures ($\epsilon_3 = \epsilon_1$) the nonreciprocity is not present.

The first- and third-order terms of the nonreciprocal contributions in Eq. (1) suggest that each one of them will dominate in different ranges of magnitudes of k_x. For small values of $k_x \ll K_z$, i.e., at the near normal incidence, the linear term in k_x on the right hand side will dominate. Its contribution is rather trivial and can be understood as a horizontal shift of the dispersion curves (either in elliptical or hyperbolic regimes) since $k_x^2 - \alpha k_x \approx (k_x - \alpha/2)^2$, where $\alpha = \frac{\Delta_2}{\epsilon_2}\frac{a_1 a_2 a_3}{a_0}\frac{\epsilon_\perp}{\epsilon_\parallel}(\epsilon_3 - \epsilon_1)$ is a small parameter. For large values of $k_x \gg K_z$, the case of large wavenumbers that is of primary interest in the hyperbolic regime, the cubic term dominates instead.

It is instructive to mention that the nonreciprocal terms in Eq. (1) can also be described as *magnetization-induced nonlocality*[48] with the following k_x-dependent effective parameters

$$\tilde{\epsilon}_\parallel(k_x) = \epsilon_\parallel\left[1 + k_x \frac{a_0 f_1 f_2 f_3}{\epsilon_\parallel}\frac{\Delta_2}{\epsilon_2}(\epsilon_3 - \epsilon_1)\right] \quad (2a)$$

$$\tilde{\epsilon}_\perp(k_x) = \epsilon_\perp\left[\frac{1 + k_x a_0 \frac{f_1 f_2 f_3 \Delta_2}{\epsilon_\parallel \epsilon_2}(\epsilon_3 - \epsilon_1)}{1 + k_x a_0 f_1 f_2 f_3 \frac{\Delta_2 \epsilon_\perp}{\epsilon_2 \epsilon_\parallel}\left(\frac{\epsilon_3}{\epsilon_1} - \frac{\epsilon_1}{\epsilon_3}\right)}\right]. \quad (2b)$$

The difference between this magnetization induced *nonreciprocal nonlocality* and the reciprocal nonlocality in conventional HMMs is that the effective parameters are odd functions of the wave-vector components.[48]

Nonreciprocal hyperbolic regimes. Figure 1 shows the effect of the nonreciprocal corrections to the effective medium parameters $\tilde{\epsilon}_{\parallel}(k_x)$ and $\tilde{\epsilon}_{\perp}(k_x)$ for two opposite propagation directions, $k_x = 15 \times k_0$ and $k_x = -15 \times k_0$. As can be seen from Fig. 1(b), the effect of the nonreciprocal corrections while being negligible for $\tilde{\epsilon}_{\parallel}(k_x)$, is significant for $\tilde{\epsilon}_{\perp}(k_x)$. Figure 1(b) shows that $\tilde{\epsilon}_{\perp}(k_x)$ has a pole near the wavelength λ=360 nm, and the shape of the curve near this pole strongly depends on the sign of k_x, i.e., on the propagation direction. Another peculiarity occurs near λ=450 nm, where $\tilde{\epsilon}_{\perp}$ exhibits additional variations which are also direction dependent. These are related to the *epsilon-near-zero* ($\epsilon_{\parallel} \approx 0$) condition and originate in the presence of $\epsilon_{\parallel}$ in the nonreciprocal terms in Eqs. (1) and (2). One of the most interesting consequences of nonreciprocity is that near such a pole the metamaterial can exhibit effective permittivities of the opposite sign for the two opposite propagation directions, i.e., $\tilde{\epsilon}_{\perp} > 0$ for the forward propagation $k_x > 0$, and $\tilde{\epsilon}_{\perp} < 0$ for the backward propagation $k_x < 0$, or vice versa, as illustrated by Fig. 1(c). The two hyperbolic regimes that occur in the structure, Type-II regime at longer wavelengths and Type-I regime for shorter wavelengths, are spectrally shifted for opposite directions of propagation. As a result, the onsets of the hyperbolic regimes for forward and backward propagating waves take place at different wavelengths.

To illustrate such nonreciprocal hyperbolic regimes we first examine the metamaterial at the wavelength $\lambda = 455$ nm, which exhibits an elliptical regime $\{\tilde{\epsilon}_{\parallel} > 0, \tilde{\epsilon}_{\perp} > 0\}$ in the absence of magnetization. Figure 2 shows changes in the dispersion as the off-diagonal component of the metal's permittivity Δ_2 gradually increases, which is equivalent to an increase in magnetization. It can be seen from Fig. 2(a) that the isofrequency contours acquire progressively more asymmetric shapes for larger values of Δ_2, ultimately leading to *a complete change in their topology*.

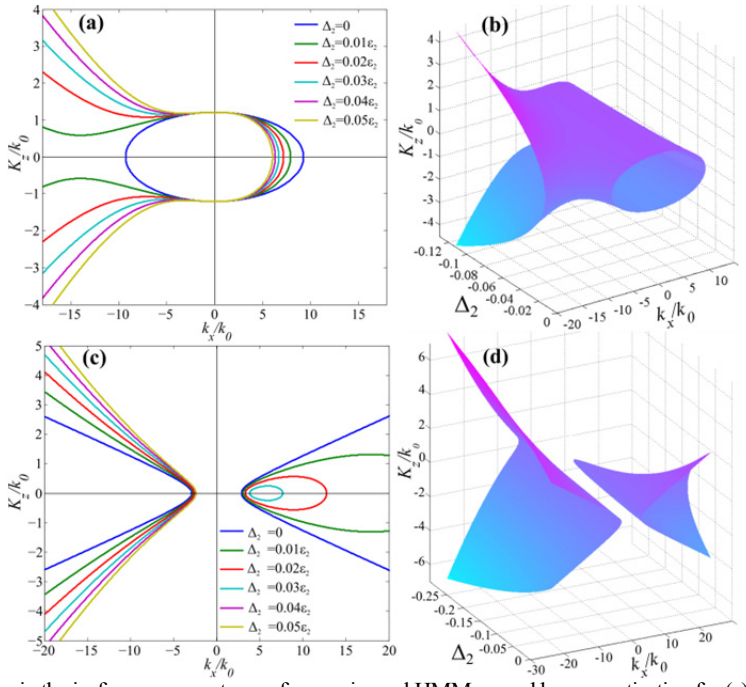

FIG. 2 (color online). Changes in the isofrequency contours of nonreciprocal HMM caused by magnetization for (a) λ =455 nm and (c) λ =360 nm. The corresponding isofrequency surfaces plotted in k_x-K_z- Δ space in (b) and (d). The structure parameters are the same as in Fig. 1. The effect of loss is not considered for the moment.

This magnetization induced *topological transition* is more clearly revealed in Fig. 2(b), which shows how one side of the closed elliptical contour ($k_x < 0$) gradually changes to an open Type-II hyperbolic contour $\{\tilde{\epsilon}_{\parallel} < 0, \tilde{\epsilon}_{\perp} > 0\}$, while the opposite side ($k_x > 0$) of the contour remains elliptical.

Next, we will study the effect of magnetization on the metamaterial at the wavelength $\lambda = 360$ nm, which in the absence of magnetization corresponds to a Type-I hyperbolic regime $\{\tilde{\epsilon}_{\parallel} > 0, \tilde{\epsilon}_{\perp} < 0\}$. Figure 2(c) shows that as in the previous case, the contours become progressively more asymmetric in shape as Δ_2 increases. In particular, the left-side of the hyperbola ($k_x < 0$), opens wider, but maintains its original topology. The right side ($k_x > 0$), in contrast, experiences a topological transition from an

open hyperbola to a closed ellipse, which eventually collapses to a point when the MO parameter reaches a critical value of $\Delta_{cr} \equiv \Delta_2 \approx 0.04\epsilon_2$, beyond which only the backward propagation is possible. This *magnetization induced topological transition* is further illustrated by Fig. 2(d): the right hyperbolic contour $k_x > 0$ gradually morphs into the isolated ellipse (tube), which then collapses to a single point and finally disappears leading to *the one-way hyperbolic regime*.

To summarize, we demonstrate and identify three distinct nonreciprocal hyperbolic regimes. The first regime – *the nonreciprocal two-way hyperbolic regime* – is characterized by the contours consisting of two asymmetric hyperbolas (for both $k_x < 0$ and $k_x > 0$), topologically equivalent to that of nonmagnetic Type-I structure (Fig. 2(c)). The second regime – *the forward-elliptical and backward-one-way hyperbolic regime* – is characterized by a hyperbola for $k_x < 0$ and an ellipse for $k_x > 0$. This regime can be subdivided into two classes corresponding to Type-I or Type-II hyperbolic regimes. In the case of Type-I hyperbolic regime, in addition to the hyperbolic branch, we encounter a closed and isolated ellipse of an asymmetric shape (Fig. 2(c)), whereas for Type-II there is half an ellipse connected to a hyperbola (Fig. 2(a)). The third regime – *the complete one-way hyperbolic regime* – appears with the further increase of the magnetization for the Type-I HMM (Fig. 2(c)) when the ellipse corresponding to $k_x > 0$ collapses.

It is important mention here that while in our calculations we used particular thickness of the layers to be 14/20/14 nm in the unit cell, due to the fact that all the dimensions are much smaller than the wavelength of light and electromagnetic waves perceives the hyperbolic metamaterial as homogenized, the response is expected to be tolerant to deviations from the precise thicknesses in both transverse and longitudinal direction. Indeed, growth of multiple layers with nanoscale precision is not easily feasible, and the layers typically vary in their thickness both within the same layer and among different layers within the stack. However, as long as we can ensure the desirable volume fraction on average, the response of the metamaterial will remain the same, which has also been evidenced by the experimental studies [43,44].

Role of magneto-plasmons in nonreciprocal hyperbolic dispersion. The hyperbolic dispersion originates from the coupling of surface plasmon polaritons (SPPs) supported by individual plasmonic layers comprising HMMs. Nonreciprocal hyperbolic regimes described here have the same origin, with the difference that the coupling takes place between surface magneto-plasmons, i.e., surface plasmons whose dispersion is modified by magnetization. To further reveal the origin of nonreciprocal and one-way hyperbolic dispersion predicted by the effective medium theory Eqs. (1) and (2), and to make predictions for realistic structures, we will now examine the eigenmodes and the transmission spectra calculated with the exact transfer matrix technique[47] for a finite layered system.

Natural plasmonic modes of layered structures are known to manifest themselves as poles in the transmission spectra and can clearly be seen in Figs. 3(a-b). Figure 3a shows the case of a single metal film (one unit cell of the HMM) where such poles form two continuous (low-frequency and high-frequency) dispersion curves corresponding to two magneto-plasmons that are predominantly localized on opposite metal-dielectric interfaces. These modes are separated by a frequency gap originating from the asymmetric cladding of the metal layer ($\epsilon_1 \neq \epsilon_3$). Note that a similar gap also exists in the dispersion of the so-called "short-range" and "long-range" plasmons in structures with an inversion symmetric unit cell. However, in the latter case the gap originates from the coupling of the plasmons on two opposite interfaces. In the case of the asymmetric cladding considered here such coupling between plasmons still exists, but is significantly suppressed due to the mismatch in their eigenfrequencies. More importantly, the dispersion of the magneto-plasmons exhibits nonreciprocity $\lambda(\boldsymbol{k}) \neq \lambda(-\boldsymbol{k})$, and in contrast to non-magnetic case, *the curves approach different asymptotes* (indicated by dashed horizontal lines) for the forward ($k_x > 0$) and backward ($k_x < 0$) propagating waves. As it is shown below, this nonreciprocity of the magneto-plasmons of the individual unit cell is the source of the nonreciprocal hyperbolic regimes found in multilayered structures.

As the next step, we consider a structure consisting of 10 unit cells with its magneto-plasmonic bands plotted in Fig. 3(b). As expected, the number of modes increases and the modes tend to push each other to the domains of longer wavenumbers and shorter wavelengths, indicating onset of the hyperbolic regimes. One can immediately establish a correspondence between the results of the effective medium theory outlined above and the exact calculations presented in Fig. 3(b). Thus, the Type-I (Type-II) hyperbolic regime occurs due to hybridization of the high frequency (low frequency) surface magneto-plasmons of the individual metal layers. The short-wavelength Type-I and long-wavelengths Type-II regimes appear to be separated by the region of elliptical dispersion. Added to this, in agreement with the effective medium calculations, the modes appear to be strongly nonreciprocal. It is worth noting that despite the hybridization of the magneto-plasmons of individual metal layers, all of the modes of multilayered structure are still approaching the same asymptotes as in the case of the single unit cell. As a result, the corresponding hyperbolic bands have different "cut-off" wavelengths for the opposite propagation directions, explaining the origin of one-way hyperbolic regimes. In particular, there is a frequency window, from $\lambda \approx$ 450 nm to $\lambda \approx$480 nm, where Type-II one-way hyperbolic regime is realized, and another window from $\lambda \approx$350 nm to $\lambda \approx$365 nm where Type-I one-way hyperbolic regime occurs.

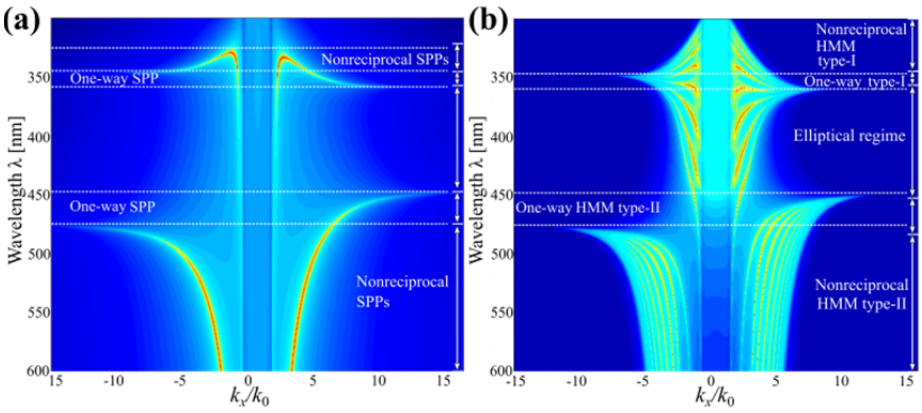

FIG. 3 (color online). Poles of the transmission through (a) single unit cell (one metal layer in asymmetric cladding) and (b) 10-unit cells of the HMM showing the dispersion of the magneto-plasmonic eigenmodes and indicating distinct nonreciprocal regimes. The geometry and material parameters are the same as in Fig.1.

Broadband nonreciprocity. From subwavelength resolution to enhanced lasing efficiency, the hyperbolic dispersion enables many fascinating applications, all made possible by the presence of plasmonic modes with very long wavenumbers.[34-44] Another advantage of HMMs is the non-resonant origin of their unique response, which amounts to the broadband character of the hyperbolic regime. This makes the HMMs very promising for various applications where broadband characteristics are required. Similar arguments can apparently be applied to nonreciprocal photonic devices. Indeed, the broadband nonreciprocal response can be achieved only in bulky optical components. To our best knowledge, all attempts to reduce the footprint of nonreciprocal devices to make them more compatible with the contemporary integrated photonic components have so far relied on the use of resonant effects.[18-26] While resonances do allow enhancement of the nonreciprocal response, they also significantly reduce the operational bandwidth of the devices. Here we show that the nonreciprocal HMMs do not have this limitation and may offer nonreciprocal response over a broad operational bandwidth.

Figure 4(a) shows transmission through the metamaterial (10 unit cells) in the Type-II hyperbolic regime for forward and backward propagation. A nonreciprocal transmission indeed occurs in the broad spectral window defined by the offset $\Delta\omega$ of the forward and backward transmission bands. The bandwidth of one-way response is defined by the difference in the cut-off frequencies for the forward and backward hyperbolic transmission bands in Fig. 3, which, in turn, is defined by the strength of magnetization. Thus, the bandwidth of the one-way response is only limited by the strength of magnetic field and MO response of the materials constituting the structure, which is in sharp contrast to the bandwidth-limited nonreciprocal devices based on resonant MO structures. In resonant structures the optical isolation (one-way response) relies on MO-induced splitting of a narrow resonance of bandwidth Γ for forward and backward propagation directions, by the extent that the splitting $\Delta\omega$ exceeds the bandwidth ($\Delta\omega > \Gamma$).[16] As a result, Lorentzian-shaped one-way transmission occurs over Γ-wide band. In contrast to this principle of operation, the nonreciprocal HMM provides a nearly uniform transmission over the entire frequency range $\Delta\omega$ (Fig. 4(a)). As with a sufficient number of layers the hyperbolic transmission bands can be made arbitrarily wide, one can always design a nonreciprocal device with the maximally possible bandwidth $\Delta\omega$.

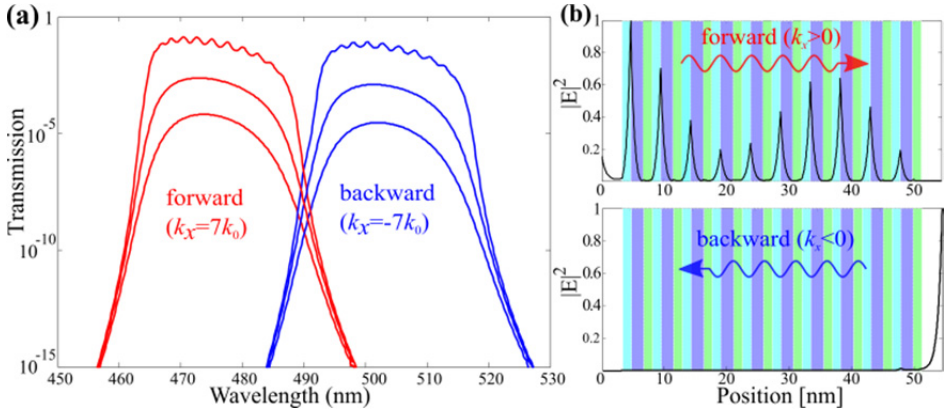

FIG. 4 (color online). (a) Transmission spectrum and (b) the field distribution at λ=470 nm for the forward ($k_x = 7k_0$) and backward ($k_x = -7k_0$) propagation directions calculated by the transfer matrix technique for the HMM consisting of 10 unit cells (metal layers are shown in purple). The material parameters used are the same as in Fig.1, and in subplot (a) the damping frequency is changed from $\gamma = 1.13\times10^{13}$ [rad/s] to $\gamma = 2.83\times10^{13}$ [rad/s] to $\gamma = 5.65\times10^{13}$ [rad/s].

The origin of the nonreciprocity can also be understood from the electric field distribution inside the HMM. The field distribution, calculated for the wavelength $\lambda = 470$ nm, is plotted in Fig. 4(b) for forward ($k_x = 7k_0$) and backward ($k_x = -7k_0$) propagation directions. The transmission in the forward direction occurs due to the excitation of the side-coupled surface plasmons (on the left side of metallic layers) propagating along the layers in the forward direction ($k_x > 0$), which transfer the electromagnetic energy through the structure. On the other hand, when excited from the opposite side with the backward propagation direction ($k_x < 0$), the excitation wavelength exceeds the cut-off wavelength ($\lambda_0 = 480$ nm) and no plasmonic modes are excited, resulting in the fast decay of the field inside the structure and vanishingly small transmission.

As for any other plasmonic structure, Ohmic losses will play a detrimental role for operation of the nonreciprocal HMM. For example, Fig. 4(a) shows how the transmission through the metamaterial changes with the increase of the damping frequency from that in the epitaxially grown silver to the thermally evaporated one.[49] As can be seen from Fig. 4(a), while the bandwidth of the nonreciprocal response stays nearly unchanged or even decreases, the transmission drops. To avoid this decrease in the transmission, the number of layers in the HMM should be reduced as shown in Supplementary Materials[47] (section 3). However, this may also lead to the narrowing in the bandwidth of the hyperbolic transmission band. Therefore, in addition to the strength of the MO response, the limitation in the operational bandwidth of nonreciprocal HMM devices will be also dictated by losses. Nevertheless, it is apparent that the operational bandwidth of HMM can always be made superior to that of resonant plasmonic structures where losses have even more detrimental effects (see Supplementary Materials[47], section 3). Moreover, the field profiles Fig. 4(b) suggest another class of applications which are possible even for strongly absorbing structures, such as nonreciprocal and one-way absorbers. The magneto-plasmons in the nonreciprocal HMMs are excited only for one direction, which implies that the absorption of incident wave will take place only in this particular direction, while a complete reflection will occur for the other.

Conclusions. We demonstrated the possibility of nonreciprocal light transmission using magnetoplasmonic hyperbolic metamaterials. New nonreciprocal hyperbolic regimes and one-way topological transitions between hyperbolic and elliptical dispersion regimes were revealed. Thanks to the non-resonant nature of the metamaterial, previously unachievable broadband nonreciprocal transmission was demonstrated which makes this design principle promising for practical applications. In addition to the visible domain studied here, the results presented hold a great potential for applications at the infrared and terahertz frequencies where nonreciprocal hyperbolic metamaterials are made of highly doped semiconductors.

Aknowledgments. This work was supported by the National Science Foundation (CMMI-1537294 and EFRI-1641069).

[1] J. B. Pendry, "Negative refraction makes a perfect lens," Phys. Rev. Lett. **85**, 3966 (2000).
[2] D.R. Smith, J.B. Pendry, and M.C.K. Wiltshire, "Metamaterials and Negative Refractive Index," Science **305**, 788 (2004).
[3] V. M. Shalaev, "Optical negative-index metamaterials," Nat. Photonics **1**, 41 (2007).
[4] Engheta, N. and R.W. Ziolkowski, *Metamaterials: physics and engineering explorations*, (Wiley & Sons New Jersey, 2006).
[5] A. K. Sarychev and V.M. Shalaev, *Electrodynamics of Metamaterials*, (World Scientific, Singapore 2007).
[6] W. Cai and V. Shalaev, *Optical Metamaterials: Fundamentals and Applications*, (Springer, Berlin 2009).
[7] R. J. Potton, "Reciprocity in optics," Rep. Prog. Phys. **67**, 717 (2004).
[8] D. Jalas, A. Petrov, M. Eich, W.Freude, S. Fan, Z. Yu, R. Baets, M. Popović, A. Melloni, J. D. Joannopoulos, M. Vanwolleghem, C. R. Doerr, H. Renner, "What is – and what is not – an optical isolator," Nat. Photonics **7**, 579 (2013).
[9] H. A. Haus, *Waves and Fields in Optoelectronics*, (Prentice-Hall, 1984).
[10] B. E. A. Saleh and M. C. Teich, *Fundamentals of Photonics*, (Wiley-Interscience, 2007).
[11] L. D. Tzuang, K. Fang, P. Nussenzveig, S. Fan, and M. Lipson, "Non-reciprocal phase shift induced by an effective magnetic flux for light," Nat. Photonics **8**, 701 (2014).
[12] M. Inoue, K. Arai, T. Fujii, and M. Abe, "One-dimensional magnetophotonic crystal," J. Appl. Phys. **85**, 5768 (1999).
[13] A. Figotin and I. Vitebskiy, "Nonreciprocal magnetic photonic crystals," Phys. Rev. E **63**, 066609, (2001).
[14] Z. Wang and S. Fan, "Optical circulators in two-dimensional magneto-optical photonic crystals," Opt. Lett. **30**, 1989–1991 (2005).
[15] Z. Yu, Z. Wang, and S. Fan, "One-way total reflection with one-dimensional magneto-optical photonic crystals," Appl. Phys. Lett. **90**, 121133 (2007).

[16]A. B. Khanikaev and M. J. Steel, "Low-symmetry magnetic photonic crystals for nonreciprocal and unidirectional devices," Opt. Express **17**, 5265 (2009).
[17]A.B. Khanikaev, A.V. Baryshev, M. Inoue, and Yu. S. Kivshar', "One-way electromagnetic Tamm states in magnetophotonic structures," Appl. Phys. Lett. **95**, 011101 (2009).
[18]V. I. Belotelov, L. L. Doskolovich, and A. K. Zvezdin, "Extraordinary Magneto-Optical Effects and Transmission through Metal-Dielectric Plasmonic Systems," Phys. Rev. Lett. **98**, 077401 (2007).
[19]A. B. Khanikaev, A. V. Baryshev, A. A. Fedyanin, A. B. Granovsky, and M. Inoue, "Anomalous Faraday effect of a system with extraordinary optical transmittance," Opt. Express **15**, 6612 (2007).
[20]Z. Yu, G. Veronis, Z. Wang, and S. Fan, "One-Way Electromagnetic Waveguide Formed at the Interface between a Plasmonic Metal under a Static Magnetic Field and a Photonic Crystal," Phys. Rev. Lett. **100**, 023902 (2008).
[21]G. A. Wurtz, W. Hendren, R. Pollard, R. Atkinson, L. Le Guyader, A. Kirilyuk, Th. Rasing, I. I. Smolyaninov, and A. V. Zayats, "Controlling optical transmission through magneto-plasmonic crystals with an external magnetic field," New J. Phys. **10**, 105012 (2008).
[22]A. B. Khanikaev, H. Moussavi, G. Shvets, and Yu. S. Kivshar, "One-way extraordinary optical transmission and nonreciprocal spoof plasmons," Phys. Rev. Lett. **105**, 126804 (2010).
[23]A. Davoyan and N. Engheta, "Nonreciprocal Rotating Power Flow within Plasmonic Nanostructures," Phys. Rev. Lett. 111, 047401 (2013).
[24]A. R. Davoyan and N. Engheta, "Nanoscale plasmonic circulator," New J. Phys. **15**, 083054 (2013).
[25]J. Y. Chin, T. Steinle, T. Wehlus, D. Dregely, T. Weiss, V. I. Belotelov, B. Stritzker, H. Giessen, "Nonreciprocal plasmonics enables giant enhancement of thin-film Faraday rotation," Nat. Commumications (2013). DOI:10.1038/ncomms2609
[26]U. K. Chettiar, A.R. Davoyan, and N. Engheta, "Hotspots from nonreciprocal surface waves," Opt. Lett. **39**, 1760-1763 (2014).
[27]S. H. Mousavi, A. B. Khanikaev, J. Allen, M. Allen, and G. Shvets, "Gyromagnetically induced transparency of Metasurfaces," Phys. Rev. Lett. **112**, 117402 (2014).
[28]H. Zhao, J. Zhou, Q. Zhao, B. Li, L. Kang, and Y. Bai, "Magnetotunable left-handed material consisting of yttrium iron garnet slab and metallic wires," Appl. Phys. Lett. **91**, 131107 (2007).
[29]F. J. Rachford, D. N. Armstead V. G. Harris, and C. Vittoria, "Simulations of Ferrite-Dielectric-Wire Composite Negative Index Materials," Phys. Rev. Lett. **99**, 057202 (2007).
[30]L. Kang, Q. Zhao, H. Zhao, and J. Zhou, "Magnetically tunable negative permeability metamaterial composed by split ring resonators and ferrite rods," Opt. Express **16**, 8825 (2008).
[31]W. Li, Z. Liu, X. Zhang, and X. Jiang, "Switchable hyperbolic metamaterials with magnetic control," Appl. Phys. Lett. **100**, 161108 (2012).
[32]K. Bi, J. Zhou, H. Zhao, X. Liu, and C. Lan, "Tunable dual-band negative refractive index in ferrite-based metamaterials," Opt. Express **21**, 10746 (2013).
[33]Y. G. Huang, G. Wen, W. Zhu, J. Li, L. M. Si, M. Premaratne, "Experimental demonstration of a magnetically tunable ferrite based metamaterial absorber," Opt. Express **22**, 16408 (2014).
[34]Z. Jacob, L. V. Alekseyev, and E. Narimanov, "Optical Hyperlens: Far-field imaging beyond the diffraction limit," Opt. Express **14**, 8247 (2006).
[35]Z. Liu, H. Lee, Y. Xiong, C. Sun, and X. Zhang, "Far-field optical hyperlens magnifying sub-diffraction-limited objects," Science **315**, 1686 (2007).
[36]A. J. Hoffman, L. Alekseyev, S. S. Howard, K. J. Franz, D. Wasserman, V. A. Podolskiy, E. E. Narimanov, D. L. Sivco, and C. Gmachl, "Negative refraction in semiconductor metamaterials," Nat. Mater. **6**, 946 (2007).
[37]M. A. Noginov, H. Li, Yu. A. Barnakov, D. Dryden, G. Nataraj, G. Zhu, C. E. Bonner, M. Mayy, Z. Jacob, and E. E. Narimanov, "Controlling spontaneous emission with metamaterials," Opt. Lett. **35**, 1863 (2010).
[38]Z. Jacob, J. Y. Kim, G. V. Naik, A. Boltasseva, E. E. Narimanov, V. M. Shalaev, "Engineering photonic density of states using metamaterials," Appl. Phys. B **100**, 215 (2010).
[39]A. N. Poddubny, P. A. Belov, and Y. S. Kivshar, "Spontaneous radiation of a finite-size dipole emitter in hyperbolic media," Phys. Rev. A 84, 023807 (2011).
[40]O. Kidwai, S. V. Zhukovsky, and J. E. Sipe, "Dipole radiation near hyperbolic metamaterials: Applicability of effective-medium approximation," Opt. Lett. **36**, 2530 (2011).
[41]V. Drachev, V. A. Podolskiy, and A. V. Kildishev, "Hyperbolic Metamaterials: new physics behind a classical problem," Opt. Express **21**, 15048 (2013).
[42]C. L. Cortes, W. Newman, S. Molesky, and Z. Jacob, "Quantum nanophotonics using hyperbolic metamaterials," J. Opt. **14**, 063001 (2012).

[43]H. N. S. Krishnamoorthy, Z. Jacob, E. Narimanov, I. Kretzschmar, and V. M. Menon, "Topological Transitions in Metamaterials," Science **336**, 205 (2012).
[44]A. Poddubny, I. Iorsh, P. Belov, and Y. Kivshar, "Hyperbolic metamaterials," Nat. Photonics **7**, 948 (2013).
[45] T. Xu and H. J. Lezec, "Visible-frequency asymmetric transmission devices incorporating a hyperbolic metamaterial," Nat. Comm. **5**, 4141 (2014).
[46] D. Jalas, A. Petrov, M. Eich, W. Freude, S. Fan, Z. Yu, R. Baets, M. Popović, A. Melloni, J. D. Joannopoulos, M. Vanwolleghem, C. R. Doerr, H. Renner, "What is - and what is not - an optical isolator," Nat. Photon. **7**, 579 (2013).
[47]See the Supplementary Materials [link] which includes Ref. [48], for details of analytic theory.
[48]J. Elser, V. A. Podolskiy, I. Salakhutdinov, and I. Avrutsky, "Nonlocal effects in effective-medium response of nanolayered metamaterials," Appl. Phys. Lett. **90**, 191109 (2007).
[49]Y. Wu, C. Zhang, N. M. Estakhri, Y. Zhao, J. Kim, M. Zhang, X. X. Liu, G. K. Pribil, A. Alù, C. K. Shih, X. Li, "Intrinsic optical properties and enhanced plasmonic response of epitaxial silver," Adv Mater. **26**, 6106 (2014).

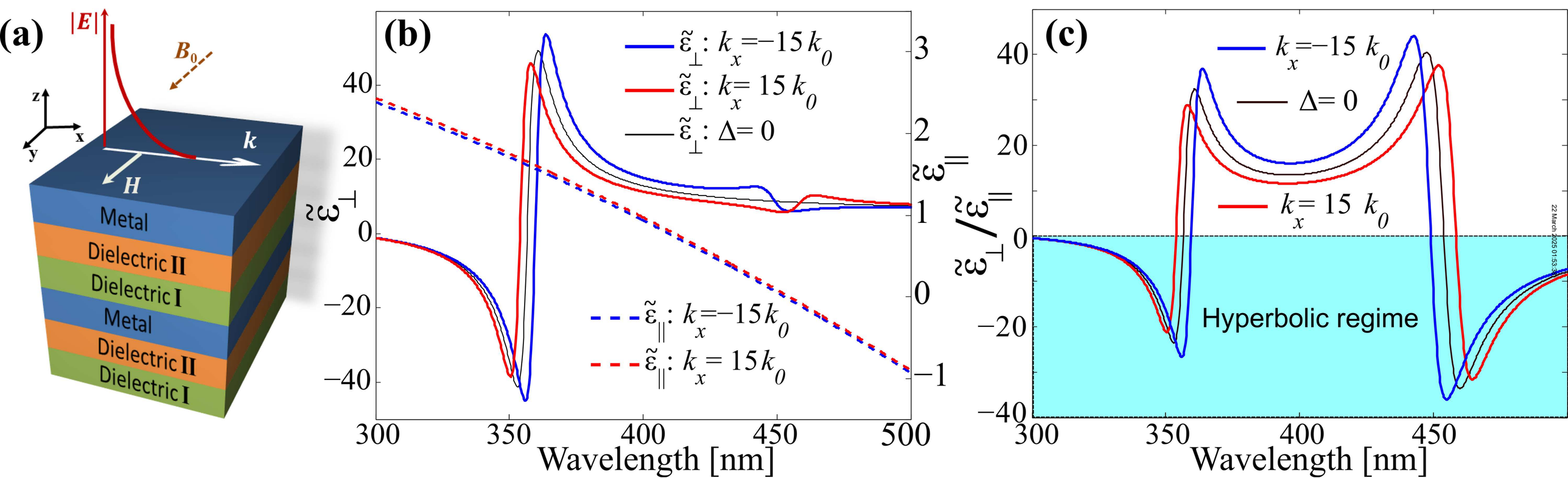
(a)
|E|
B0
z
x
y
k
H
Metal
Dielectric II
Dielectric I
Metal
Dielectric II
Dielectric I
(b)
$\tilde{\varepsilon}_\perp$: k_x=−15 k_0
$\tilde{\varepsilon}_\perp$: k_x= 15 k_0
$\tilde{\varepsilon}_\perp$: Δ= 0
$\tilde{\varepsilon}_\parallel$: k_x=−15 k_0
$\tilde{\varepsilon}_\parallel$: k_x= 15 k_0
$\varepsilon_\perp$
$\varepsilon_\parallel$
Wavelength [nm]
(c)
k_x=−15 k_0
Δ= 0
k_x= 15 k_0
$\varepsilon_\parallel/\varepsilon_\perp$
Hyperbolic regime
Wavelength [nm]
22 March 2025 01:53:38

(a)

Δ_2=0
Δ_2=0.01ε_2
Δ_2=0.02ε_2
Δ_2=0.03ε_2
Δ_2=0.04ε_2
Δ_2=0.05ε_2

K_z/k_0

k_x/k_0

(b)

K_z/k_0

Δ_2

k_x/k_0

(c)

Δ_2 =0
Δ_2 =0.01ε_2
Δ_2 =0.02ε_2
Δ_2 =0.03ε_2
Δ_2 =0.04ε_2
Δ_2 =0.05ε_2

K_z/k_0

k_x/k_0

(d)

K_z/k_0

Δ_2

k_x/k_0

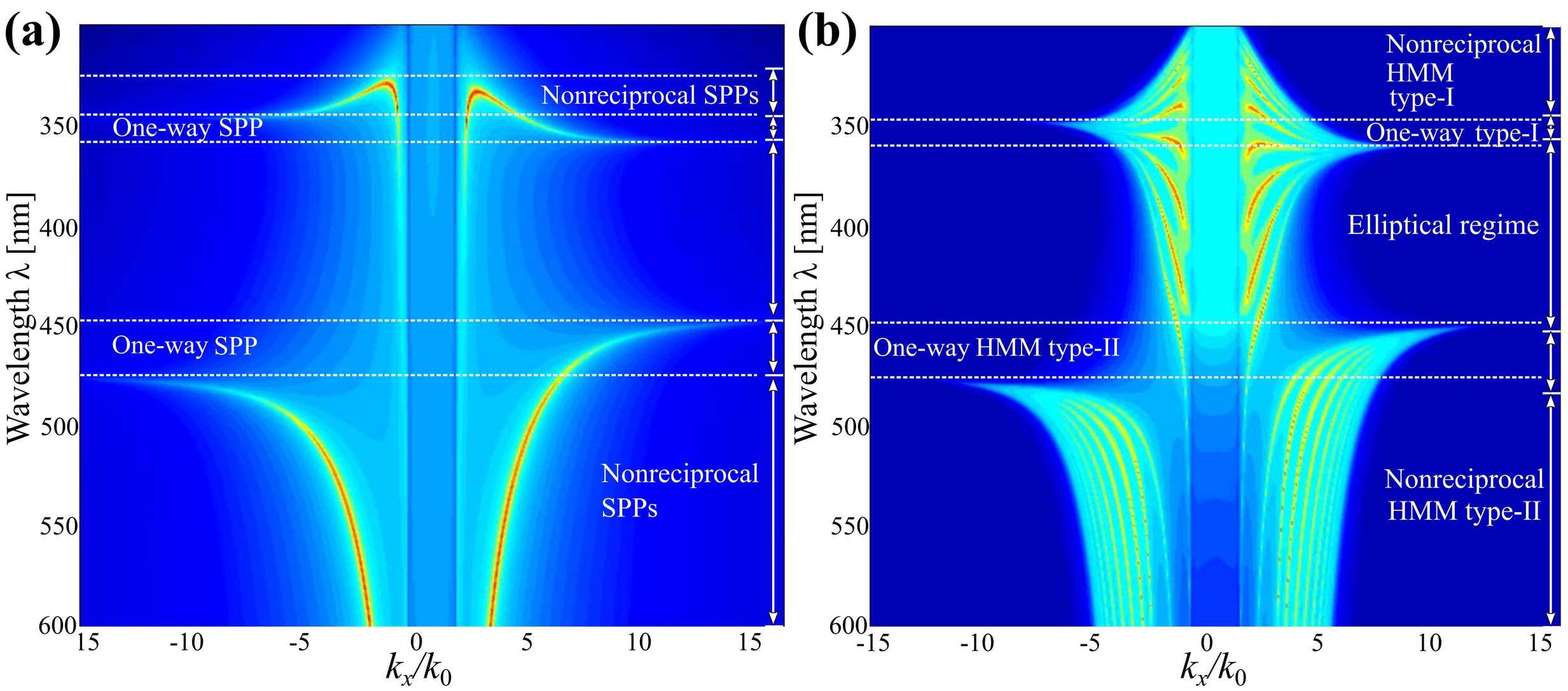
(a)
Nonreciprocal SPPs
One-way SPP
One-way SPP
Nonreciprocal SPPs
Wavelength λ [nm]
350
400
450
500
550
600
15
-10
-5
0
5
10
15
k_x/k_0
(b)
Nonreciprocal HMM type-I
One-way type-I
Elliptical regime
One-way HMM type-II
Nonreciprocal HMM type-II
Wavelength λ [nm]
350
400
450
500
550
600
-15
-10
-5
0
5
10
15
k_x/k_0

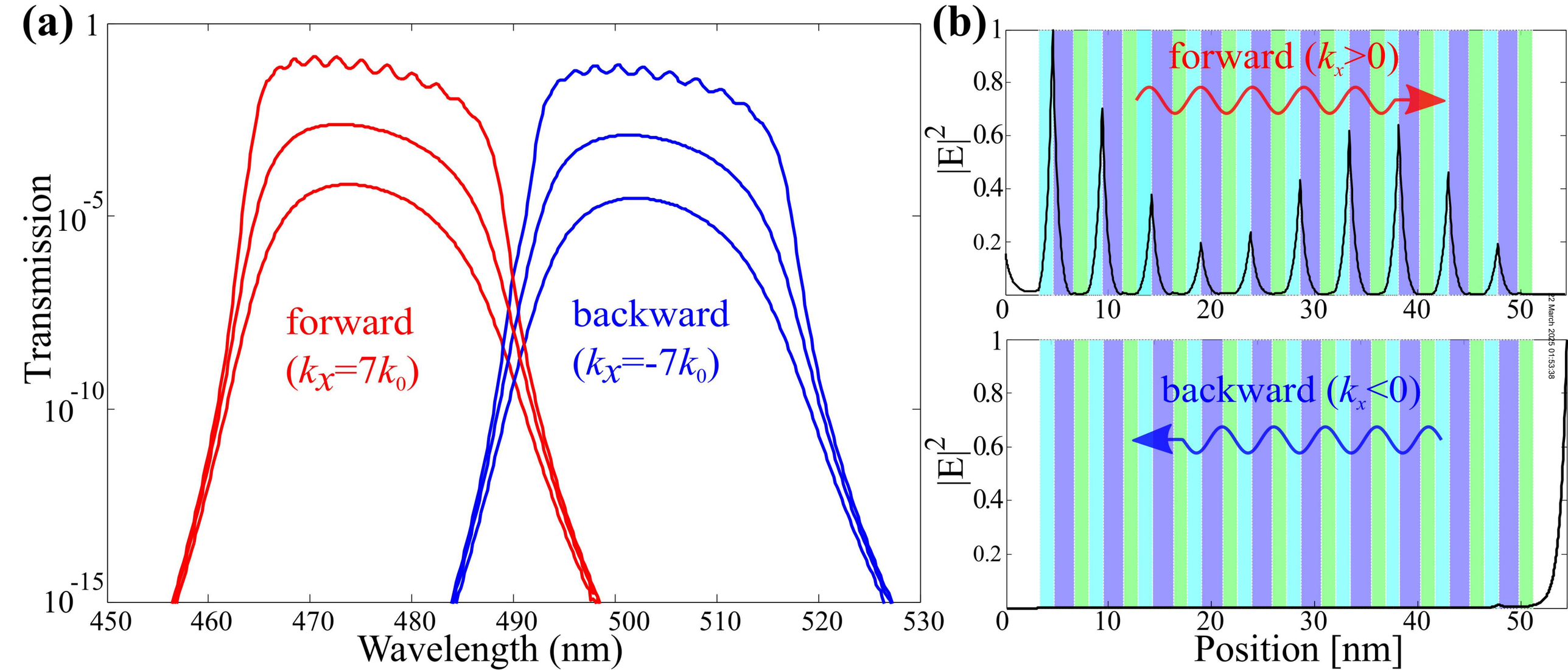
(a)
Transmission
1
10^-5
10^-10
10^-15
forward
(kx=7k0)
backward
(kx=-7k0)
450
460
470
480
490
500
510
520
530
Wavelength (nm)
(b)
|E|^2
1
0.8
0.6
0.4
0.2
forward (kx>0)
0
10
20
30
40
50
backward (kx<0)
Position [nm]
22 March 2025 01:53:38